Journal of Medicinal Chemistry

Article

Discovery and Optimization of a Novel Series of Highly Selective JAK1 Kinase Inhibitors

Neil P. Grimster, Erica Anderson, Marat Alimzhanov, Geraldine Bebernitz, Kirsten Bell, Claudio Chuaqui, Tracy Deegan, Andrew D. Ferguson, Thomas Gero, Andreas Harsch, Dennis Huszar, Aarti Kawatkar, Jason Grant Kettle, Paul D Lyne, Jon A. Read, Caroline Rivard Costa, Linette Ruston, Patricia Schroeder, Jie Shi, Qibin Su, Scott Throner, Dorin Toader, Melissa Marie Vasbinder, Richard Woessner, Haixia Wang, Allan Wu, Minwei Ye, Weijia Zheng, and Michael Zinda

J. Med. Chem., **Just Accepted Manuscript** • DOI: 10.1021/acs.jmedchem.8b00076 • Publication Date (Web): 01 Jun 2018

Discovery and Optimization of a Novel Series of Highly Selective JAK1 Kinase Inhibitors

Neil P. Grimster,[1]* Erica Anderson,[1] Marat Alimzhanov,[1] Geraldine Bebernitz,[1] Kirsten Bell,[1] Claudio Chuaqui,[1] Tracy Deegan,[1] Andrew D. Ferguson,[2] Thomas Gero,[1] Andreas Harsch,[3] Dennis Huszar,[3] Aarti Kawatkar,[1] Jason G. Kettle,[3] Paul Lyne,[1] Jon A. Read,[4] Caroline Rivard Costa,[1] Linette Ruston,[5] Patricia Schroeder,[1] Jie Shi,[1] Qibin Su,[1] Scott Throner,[1] Dorin Toader,[1] Melissa Vasbinder,[1] Richard Woessner,[1] Haixia Wang,[1] Allan Wu,[2] Minwei Ye,[1] Weijia Zheng,[1] Michael Zinda.[1]

[1]Oncology, IMED Biotech Unit, AstraZeneca, Waltham, USA. [2]Discovery Sciences, IMED Biotech Unit, AstraZeneca, Waltham, USA. [3]Oncology, IMED Biotech Unit, AstraZeneca, Cambridge, UK. [4]Discovery Sciences, IMED Biotech Unit, AstraZeneca, Cambridge, UK. [5]Pharmaceutical Sciences, IMED Biotech Unit, AstraZeneca, Macclesfield, UK.

Abstract

Janus kinases (JAKs) have been demonstrated to be critical in cytokine signaling, and have thus been implicated in both cancer and inflammatory diseases. The JAK family consists of 4 highly homologous members: JAK1,2,3 and TYK2. The development of small molecule inhibitors that are selective for a specific family member would represent highly desirable tools for deconvoluting the intricacies of JAK family biology.

Herein, we report the discovery of a potent JAK1 inhibitor, 24, which displays ~1000 fold selectivity over the other highly homologous JAK family members (determined by biochemical assays), while also possessing good selectivity over other kinases (determined by panel

screening). Moreover, this compound was demonstrated to be orally bioavailable, and possesses acceptable pharmacokinetic parameters. In an in vivo study, the compound was observed to dose dependently modulate the phosphorylation of STAT3 (a downstream marker of JAK1 inhibition).

Introduction

Janus kinases (JAKs) are critical in cytokine signaling through type I and II receptors, and have been linked to both cancer[1] and inflammatory diseases.[2] The JAK family consists of four members: JAK1, JAK2, JAK3 and tyrosine kinase 2 (TYK2), and there are currently two FDA approved JAK family inhibitors on the market: *tofacitinib* (**1**, a JAK1/3 inhibitor from Pfizer)[3] for rheumatoid arthritis, and *ruxolitinib* (**2**, a selective JAK1/2 inhibitor from Incyte/Novartis)[4] for myelofibrosis (Figure 1).

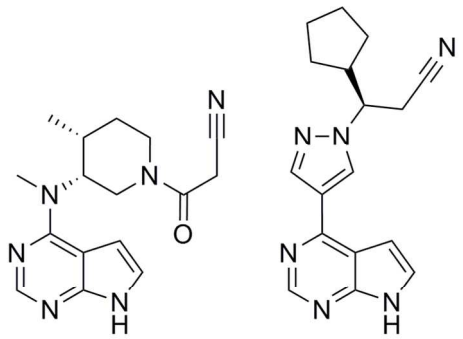

1 (Tofacitinib)
Pfizer
JAK1/3

2 (Ruxolitinib)
Incyte/Novartis
JAK1/2

Compound	JAK1 IC_{50} (μM)[a]	JAK2 IC_{50} (μM)[a]	JAK3 IC_{50} (μM)[a]
1	0.030	0.130	0.074
2	0.038	0.060	1.940

Figure 1. FDA approved JAK family inhibitors. [a] Measured in our in-house assays at 5 mM ATP concentration. All values represent the geometric mean of at least two independent experiments.

Both compounds display good efficacy in a number of disease areas, but have known on target toxicities, e.g., increased risk of infection, anemia (platelets, red and white blood cells), hypercholesterolemia, and increased transglutaminases and creatinine levels. As such, second generation inhibitors with increased levels of selectivity for JAK1 are currently under clinical evaluation.[5] The expectation is that these agents will enable better prognosis upon chronic usage, because their selectivity over JAK2 will lead to less severe hematological side effects.[6]

In oncology, the JAK/STAT pathways have been associated with a wide variety of malignancies upon constitutive activation. This can occur through autocrine and paracrine cytokine production, as well as specific activating mutations on the signaling pathway (e.g. cytokine receptors, JAKs, or STATs). Increased activation of STAT3 via phosphorylation at Y705 (pSTAT3) is reported to be elevated in a wide variety of cancers, including breast, liver, prostate, colorectal, head and neck, esophageal, pancreatic, bladder, and non-small cell lung;[7] it has also been implicated in the pathogenesis of diffuse large B-cell lymphoma[8] and nasopharyngeal carcinomas.[9] Overall, persistent elevated STAT3 activity is present in ~70% of human tumors,[10] and has been linked to poorer prognosis in many of these settings.[11] Moreover, elevation of STAT3 signaling is observed in response to both chemotherapy and treatment with oncogenic signaling pathway inhibitors e.g. EGFR, MAPK and Akt.[12] JAK1 is often the primary kinase that phosphorylates STAT3, and thus drives downstream signaling.[13] Taken together, these findings suggest that small molecule inhibition of JAK1 may offer a potential therapeutic approach toward the treatment of these resistance or "escape" mechanisms. The highly complex interplay of the JAK/STAT pathways, however, means that elucidating the precise role of JAK1 in these

processes has proved challenging. One approach to address these challenges is through the development of small molecule inhibitors of JAK1 that display a high degree of selectivity vs. the other family members.

Herein, we describe the discovery of a highly potent ATP-competitive JAK1 inhibitor. This compound displays remarkable selectivity against the other JAK family members, as well as excellent selectivity against all other kinases tested. A detailed biological and pharmacokinetic evaluation of this compound will also be described.

Chemistry

2,4-Dichloropyrimidines, differentially substituted at the C-5 position, were reacted with anilines under basic conditions to selectively displace the C-4 chloride. A subsequent acid catalyzed aniline displacement yielded the desired bis-anilino pyrimidines (For an example see **Scheme 1**).

Scheme 1. Example Synthesis of Compound 7[a]

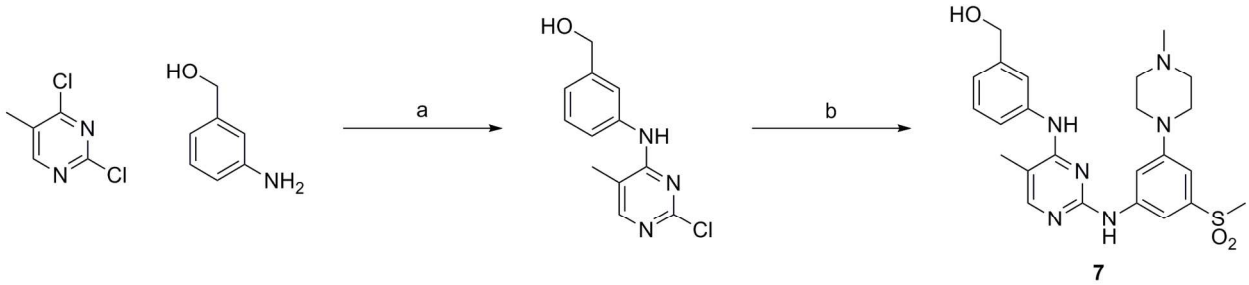

[a]Reagents and conditions: (a) $NaHCO_3$, EtOH, 80 °C, 16 h, 63 %; (b) **S14**, HCl, EtOH, 120 °C (microwave), 2 h, 36 %.

To override the inherent C-4 reactivity of the pyrimidine core, formylated anilines were deprotonated with sodium hydride and then reacted with C-2 methyl sulfone pyrimidines.[14] A subsequent basic work-up cleaved the formyl group and yielded the desired 2-anilino-4-chloropyrimidines. Substitution at the 4-position was carried out under acidic conditions in the

case of anilines, and basic conditions when alkylamines were used (For an example see **Scheme 2**).

Scheme 2. Example Synthesis of Compound 24[a]

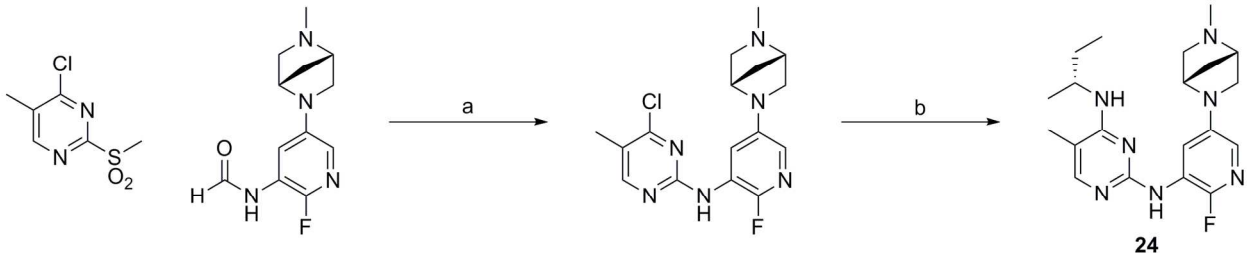

[a]Reagents and conditions: (a) NaH, THF, 40 °C, 16 h, 83% (b) (*R*)-butan-2-amine, DIPEA, butan-1-ol, 125 °C, 24 h, 69%.

Results and Discussion

SAR Development. To identify selective JAK1 inhibitors, we first screened a 50,000 membered subset of our compound collection, which was biased toward motifs known to bind the ATP binding site of kinases. Initially, three point IC_{50}s were determined, and approximately 1,400 compounds were identified as possessing an IC_{50} <100 nM against JAK1 (K_m ATP concentration, 55 μM). These compounds were subsequently re-screened in a 5 point IC_{50} format vs. JAK1, 2, and 3, at the corresponding K_m ATP concentrations (55 μM, 15 μM, and 3μM; respectively) in order to identify potent and selective starting points for further optimization. Through these efforts, we identified compound **3** from our previously described EphB4 program.[15] Compound **3** displayed excellent JAK1 biochemical potency, as well as moderate selectivity over the other JAK family members tested (**Table 1**). Interestingly, we observed that the degree of selectivity toward JAK1 appeared to be, in part, determined by the C-2 aniline, with other bis-2,4-anilino-pyrimidines, such as **4**, showing a preference for JAK2 inhibition (**Table 1**).

Table 1. Initial Screening Hits

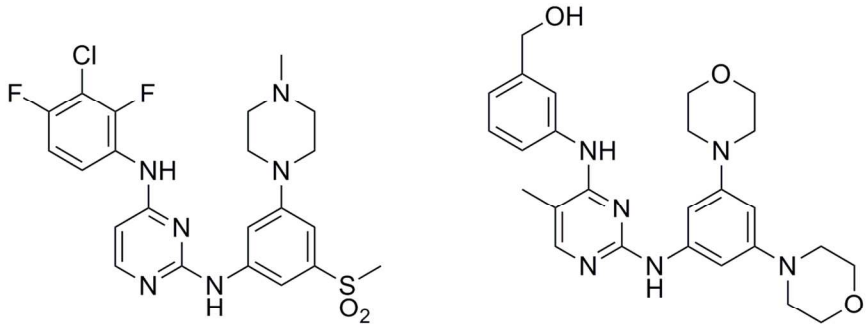

3 **4**

Compound	JAK1 IC_{50} (μM)[a]	JAK2 IC_{50} (μM)[a]	JAK3 IC_{50} (μM)[a]	Fold selectivity vs. JAK2[b]
3	<0.003	0.036	0.464	>10
4	0.004	<0.003	0.371	<0.75

[a] Measured at Km ATP concentration. All values represent the geometric mean of at least two independent experiments. For experimental details, see the Supporting Information. [b] Fold selectivity derived from JAK2/JAK1 enzyme IC_{50}. For experimental details, see the Supporting Information.

We believed that both **3** and **4** were ATP competitive inhibitors that accessed the same binding mode as previously reported,[15] i.e. the C-2 aniline of the pyrimidine was positioned toward the solvent channel. While the ATP binding sites of JAK1, 2, and 3 are highly homologous, there are key structural differences in this region; notably, the solvent channel in JAK1 is flanked by a positively charged arginine while the analogous residues in JAK2 and 3 are neutral (glutamine and serine, respectively). We hypothesized that the interaction of the methyl-sulfone of **3** with the arginine may account for its observed selectivity (JAK1 Vs. JAK2).

To test this hypothesis, we combined the C-2 aniline of **3** with the C-4 aniline of **4**, and synthesized compound **5.** Initially, we observed that under our assay conditions (K_m ATP

concentration) **5** maintained JAK1 potency (**Table 2**). Increasing the ATP concentration to a more physiologically relevant level (5 mM), reduced the IC_{50} of **5** to 100 nM vs. JAK1 (**Table 2**). Utilizing the same high ATP conditions to probe JAK2 and JAK3 activity revealed **5** to be 139 and >300 fold selective for JAK1 over JAK2 and JAK3, respectively. (**Table 2**). Moreover, replacing the highly lipophilic 3-chloro-2,4-difluoroaniline group from **3** with 3-hydroxymethylaniline from **4** had the effect of significantly lowering logD (3.11 vs. 1.75) and thus generating a more favorable starting point to begin medicinal chemistry efforts. Initially, we focused on identifying an optimal C-5 substituent of the pyrimidine ring (**5-9**, **Table 2**).

Table 2. C-5 Pyrimidine Substitution

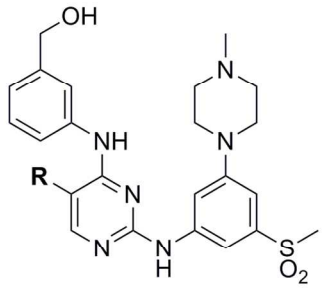

5-9

Compound	R substituent	JAK1 IC_{50} (μM)[a]	JAK2 IC_{50} (μM)[a]	JAK3 IC_{50} (μM)[a]	Fold selectivity vs. JAK2[b]	logD
5	H	<0.003[c] / 0.100	13.9	>30	140	1.75
6	F	0.042	6.41	>30	150	1.84
7	Me	<0.003	0.929	>30	>310	1.74
8	Cl	<0.003	0.722	12.6	>240	2.16
9	Br	<0.003	0.363	6.54	>120	2.43

[a] Measured at 5 mM ATP concentration. All values represent the geometric mean of at least two independent experiments. [b] Fold selectivity derived from JAK2/JAK1 enzyme IC_{50}. For experimental details, see the Supporting Information. [c] Measured at K_m ATP concentration. For experimental details, see the Supporting Information.

As can been seen in Table **2**, increasing the size of the substituent at the C-5 position led to an increase in potency for JAK1. While potency was also increased vs. JAK2, selectivity was improved for the 5-Me (**7**) and 5-Cl (**8**) substitution. We elected to continue our studies maintaining a constant C-5 methyl group, due to its acceptable balance of potency, selectivity and lipophilicity.

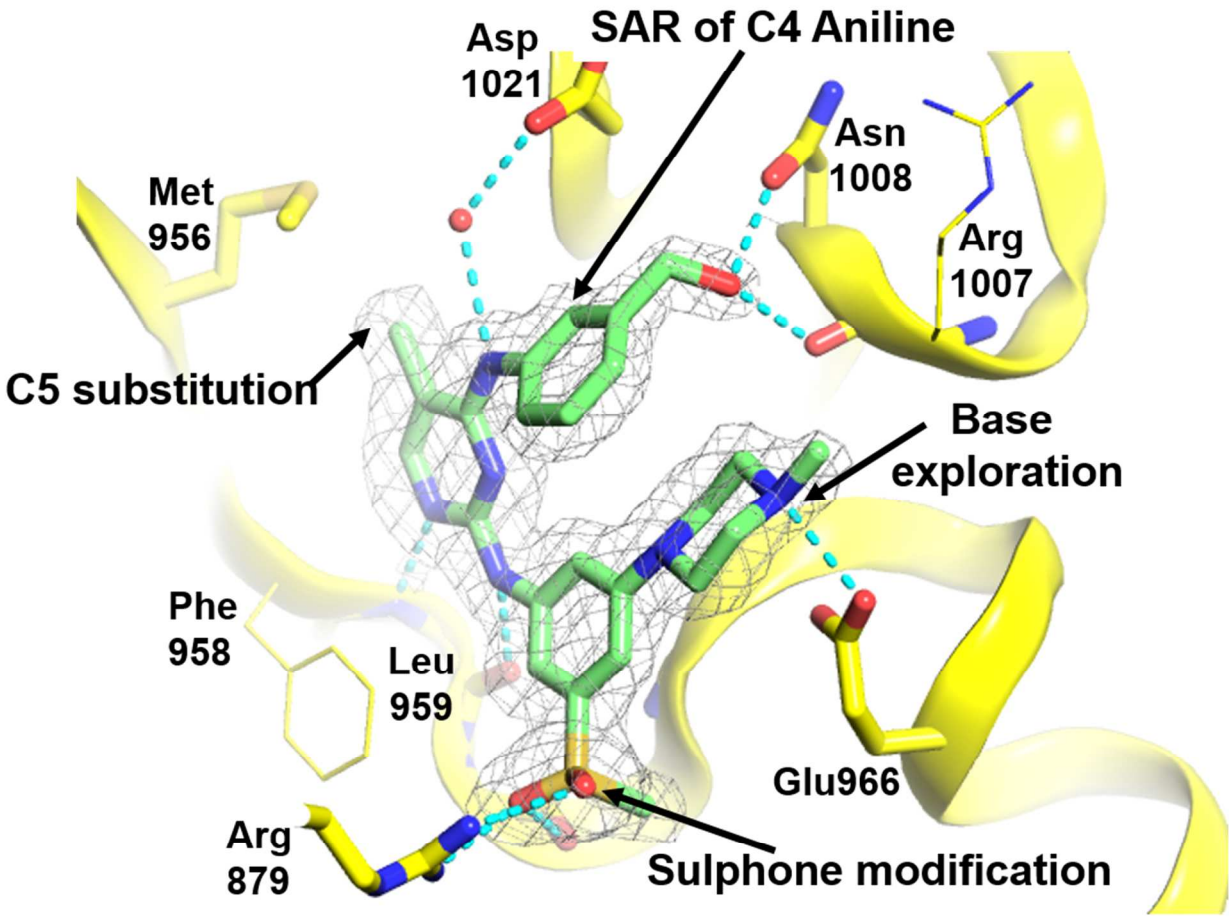

Figure 2. X-ray crystal structures of 7 (PDB ID **6ELR**) bound to the human JAK1 kinase domain. Carbon atoms for compounds are shown in green. The protein backbone cartoon is represented in yellow. Selected atoms for the JAK1 side chains are shown as sticks. Close polar contacts are represented as dotted cyan lines. Refined (2fofc) electron density contoured at 1.0 σ is represented as a wire mesh. Some atoms of the active site covering loop have been removed for clarity.

Subsequently, a co-crystal structure of **7** bound in the kinase domain of JAK1 was obtained (**Figure 2**). As expected, the aminopyrimidine core forms a hydrogen bond donor-acceptor motif with the backbone amides of the hinge region, Phe958 and Leu959; while the 5-Me substituent is positioned proximal to gatekeeper residue, Met956. The N-H of the C-4 aniline appears to interact with Asp1021 via a bridging water molecule, and the hydroxymethyl group forms a

hydrogen bond to the amide side chain of Asn1008. In the solvent channel, the *N*-methyl piperazine base and methyl sulfone generate a two-point binding interaction; the base forms a salt bridge with Glu966, while the sulfone forms a bidentate interaction with Arg879, as hypothesized. We believed that these structural features in the solvent channel may account for the observed selectivity of **7** (JAK1 vs. JAK2,3).

Having identified this two-point interaction in the solvent channel, we decided to probe the contributions of the individual components (*N*-Me piperazine and methylsulfone). To this end, compounds **10-11** were synthesized (**Table 3**) and screened against JAK1, JAK2 and JAK3. Consistent with our model that both interactions are required for potent and selective JAK1 inhibitors, replacement of the basic nitrogen with an oxygen, **10**, or removal of the sulfone moiety, **11**, resulted in a reduction in both potency and selectivity.

Table 3. Probing the Solvent Tail Interactions

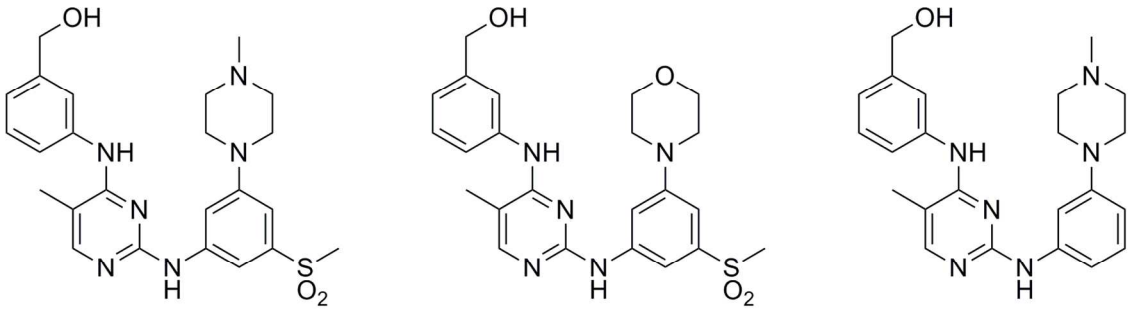

7 **10** **11**

Compound	JAK1 IC_{50} (μM)[a]	JAK2 IC_{50} (μM)[a]	JAK3 IC_{50} (μM)[a]	Fold selectivity vs. JAK2[b]	pSTAT3 EC_{50} (μM)[c]
7	<0.003	0.929	>30	>309	0.099
10	0.013	0.417	>30	32	N.D.
11	0.055	0.357	20.3	6.5	N.D.

[a] Measured at 5 mM ATP concentration. All values represent the geometric mean of at least two independent experiments. For experimental details, see the Supporting Information. [b] Fold selectivity derived from JAK2/JAK1 enzyme IC_{50}. [c] Represents cellular mode of action assay measuring inhibition of pSTAT3 in NCI-H1975 cells. For experimental details, see the Supporting Information. N. D. = not determined.

Having generated a potent JAK1 inhibitor, **7**, we were intrigued to examine whether it would show pathway modulation in a cellular setting. To this end, we developed a mode of action assay in NCI-H1975 cells, and were pleased to observe that **7** inhibited the phosphorylation of STAT3, a direct substrate of JAK1, with an EC_{50} of 99 nM (**Table 3** and **Supporting Information**). With a compound in hand capable of modulating the JAK1-STAT3 pathway, and an understanding of the structural features that govern selectivity over closely related family members, we turned our attention to its metabolic stability. We noted that **7** suffered from high *in vitro* metabolism (human liver microsomes: CL_{int} = 59.5 μl/min/mg (**Table 4**)), and believed that this may be due

to demethylation of the *N*-Me piperazine base.[16] In an attempt to address this possible metabolic hotspot, we first synthesized secondary amine **12**. While **12** maintained potency and selectivity in our biochemical assay (**Table 4**), we observed a large reduction in cellular potency. We attributed this to its poor cellular permeability, a problem that was not alleviated upon steric modulation of the secondary amine's pKA through incorporation of flanking *cis*-methyl groups, **13** (**Table 4**). Next, we removed the basic center entirely by capping it as an acetamide, **14**, and somewhat surprisingly observed only a minor drop in potency for JAK1. Unfortunately, **14** displayed a significant reduction in selectivity over JAK2. Compounds **15** and **16** attempted to modulate the basicity of the *N*-Me piperazine, but introduction of an extra hydrogen bond donor, **15**, resulted in a substantial disconnect between biochemical and cellular activity; while **16** lost potency against JAK1. Finally, we introduced a bicyclic base, **17**, which yielded similar levels of potency (biochemical and cellular) and selectivity to **7**, but was found to be more metabolically stable (human liver microsomes: CL_{int} = 7.3 vs. 59.5 μl/min/mg, respectively, **Table 4**).

Table 4. Base Optimization

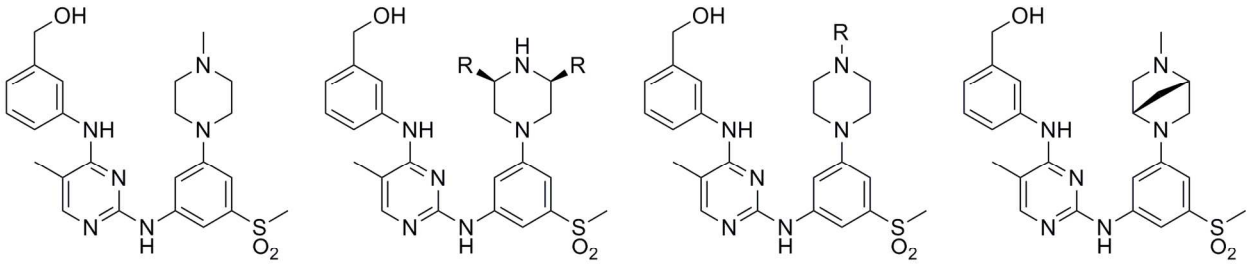

7 | 12 R = H, 13 R = Me | 14 = Ac, 15 = CH_2CH_2OH, 16 = CH_2CH_2OMe | 17

Compound	JAK1 IC_{50} (μM)[a]	JAK2 IC_{50} (μM)[a]	JAK3 IC_{50} (μM)[a]	pSTAT3 EC_{50} (μM)[b]	logD	Hu Mics CL_{int} (μl/min/mg)	PSA (Å^2)
7	<0.003	0.929	>30	0.099	1.74	59.5	109.8
12	<0.003	0.951	>30	0.496	1.09	N.D.	123.2
13	0.005	0.996	>30	0.325	1.24	N.D.	123.2
14	0.010	0.347	24.6	>3	1.74	N.D.	128.1
15	0.006	0.817	>30	>3	1.29	N.D.	132.6
16	0.012	1.03	>30	0.189	1.90	N.D.	118.6
17	<0.003	1.18	>27.9	0.092	0.82	7.32	109.8

[a] Measured at 5 mM ATP concentration. All values represent the geometric mean of at least two independent experiments. For experimental details, see the Supporting Information. [b] Represents cellular mode of action assay measuring inhibition of pSTAT3 in NCI-H1975 cells. For experimental details, see the Supporting Information. N. D. = not determined.

During optimization of the base region, we had observed that small structural changes could result in a disconnect between cellular and biochemical potency, and believed that the compounds' high polar surface area (PSA – **Table 4**) reduced their ability to traverse the cell membrane.[17] To address this issue, we synthesized **18**, which contained a di-fluoro methyl group as an isostere[18] for the highly polar methyl sulfone (**Table 5**). Pleasingly, despite observing a reduction in JAK1 biochemical potency, **18** displayed improved cellular activity (**Table 5)**. Unfortunately, this came at the expense of selectivity over other JAK family members. In an attempt to lock the conformation of **18** at the base of the solvent channel, and thereby rigidify its

two-point binding mode, we inserted an ortho-fluorine atom, **19**. Remarkably, **19** was found to be completely inactive in our biochemical assay against both JAK2 and JAK3. Unfortunately, the removal of the sulfone motif and the addition of three fluorine atoms resulted in an ~2 log unit increase in lipophilicity (measured logD **17**: 0.82 vs. **19**: 2.80), which we believed may lead to poor overall kinase selectivity. In light of this, we replaced the di-fluoro methylphenyl group with a more polar pyridine motif, **20**, which we believed may interact with Arg879 via a bridging water molecule. Pleasingly, **20** displayed good JAK1 biochemical potency and excellent JAK family selectivity. It should be noted that removal of pyridine nitrogen, **21**, maintained JAK family selectivity but at the expense of JAK1 potency, providing some evidence for the proposed water mediate interaction with Arg879, and suggesting that the placement of the fluorine atom is key to JAK family selectivity.

Table 5. Sulfone Isosteres

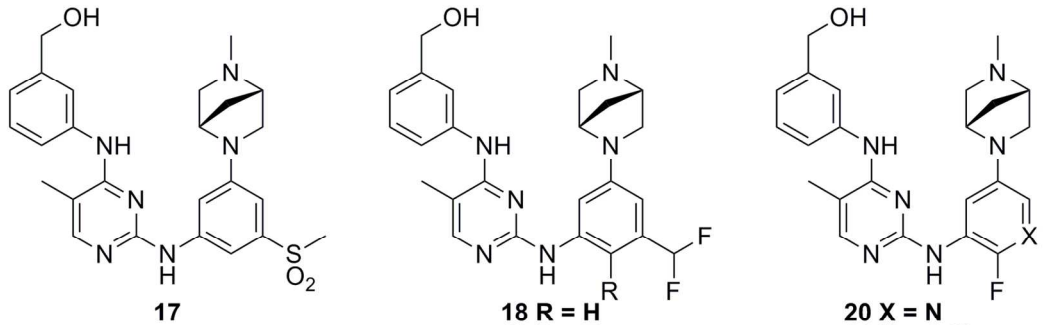

Compound	JAK1 IC_{50} (μM)[a]	JAK2 IC_{50} (μM)[a]	JAK3 IC_{50} (μM)[a]	pSTAT3 EC_{50} (μM)[b]	PSA (Å^2)	A549 GI_{50} (μM)[c]
17	<0.003	1.18	>27.9	0.092	109.8	N.D.
18	0.016	0.376	18.1	0.037	73.0	N.D.
19	0.055	>30	>30	0.026	73.0	N.D.
20	0.040	>30	>30	0.068	83.3	0.253
21	0.117	>30	>30	0.101	73.0	N.D.

[a] Measured at 5 mM ATP concentration. For experimental details, see the Supporting Information. [b] Represents cellular mode of action assay measuring inhibition of pSTAT3 in NCI-H1975 cells. [c] Represents cellular anti-proliferation assay in A549 cells. For experimental details, see the Supporting Information. N.D. = not determined.

Having designed out the sulfone group, while maintaining potency and selectivity for JAK1, we were keen to assess the off-target activity of **20**. When we evaluated it an A549 cellular proliferation assay (a cell line in which *JAK1* knockdown had no effect on cellular viability or proliferation)[19], we noted that **20** potently inhibited proliferation (GI_{50} = 0.253 μM).

We believed that to generate a truly unique tool molecule capable of probing JAK1 biology *in vivo* required further improvement in overall kinase selectivity.[5] To this end, we synthesized a diverse library of compounds which varied the C-4 substituent of **20**, installing both alkyl amines

and anilines. These compounds were evaluated for JAK1 biochemical potency and their antiproliferative effects in A549 cells. This exercise revealed several compounds which possessed high levels of JAK1 potency, but appeared inactive against our A549 assay (**Graph 1** – boxed compounds).

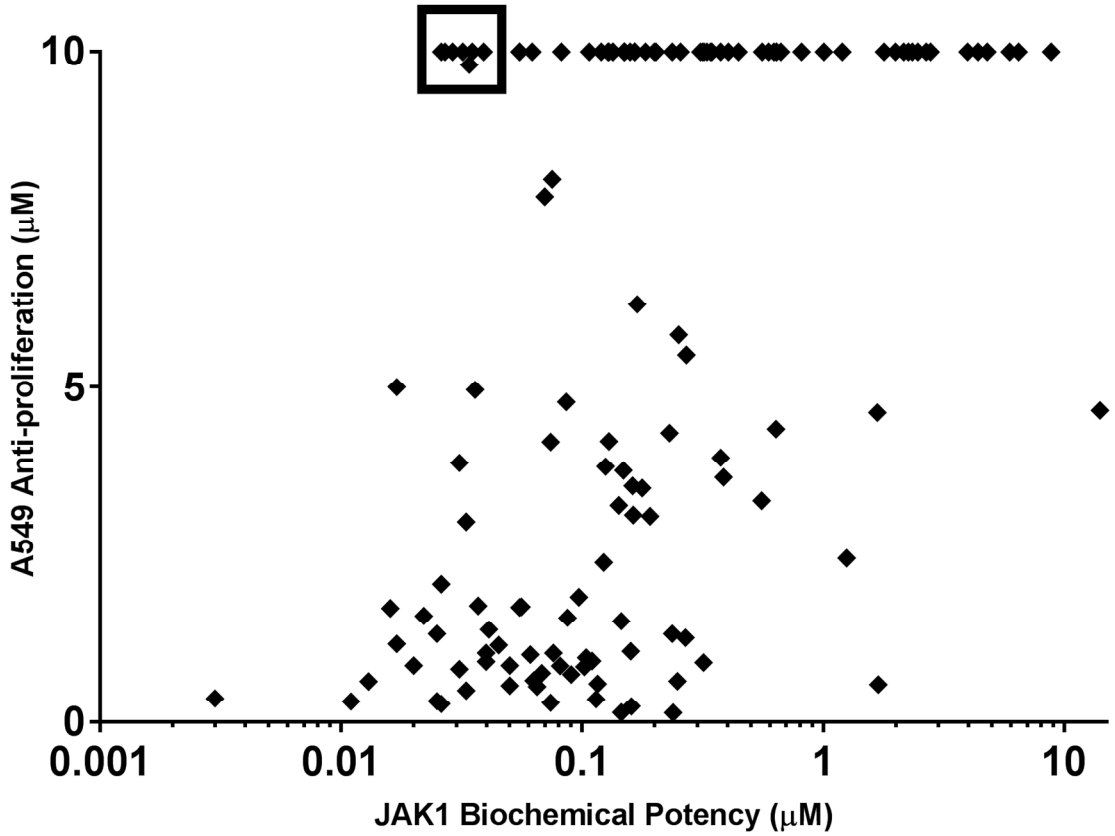

Graph 1. Plot of JAK1 biochemical potency vs. cellular anti-proliferation assay in A549 cells. Seven compounds in the black box possess potent JAK1 activity while proving inactive (>10 μM) against A549 proliferation.

Of these seven compounds, four contained highly lipophilic anilines and we thus focused our attention on the remaining three compounds (**22-24**, **Table 6**). Interestingly, all three were highly

homologous, with **22** and **24**[20] sharing a common *R* configuration at the stereogenic center. Further profiling these compounds revealed remarkably similar profiles, as may be expected. Compound **24**, however, possessed a lower logD (**24**: 2.26 vs. **22**: 2.70 **23**: 2.70), and we therefore elected to examine whether it would make an appropriate *in vivo* probe molecule.

Table 6. C-5 Alkylamine Compounds

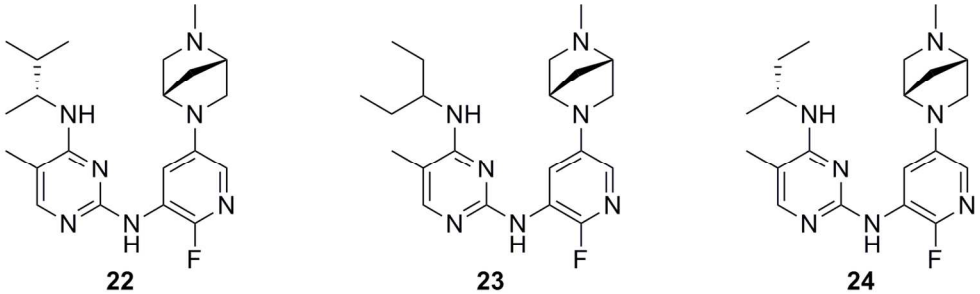

22 **23** **24 (AZ-3)**

Compound	JAK1 IC_{50} (μM)[a]	JAK2 IC_{50} (μM)[a]	JAK3 IC_{50} (μM)[a]	TYK2 IC_{50} (μM)[a]	pSTAT3 EC_{50} (μM)[b]	A549 GI_{50} (μM)[c]
22	0.026	>30	18.1	24.7	0.050	>10
23	0.029	>30	>30	>30	0.044	>10
24	0.034	>30	>30	>30	0.030	>10

[a] Measured at 5 mM ATP concentration. All values represent the geometric mean of at least two independent experiments. [b] Represents cellular mode of action assay measuring inhibition of pSTAT3 in NCI-H1975 cells. [c] Represents cellular anti-proliferation assay in A549 cells. For experimental details, see the Supporting Information.

Selectivity profile

Having already established that **24** displayed excellent selectivity against both JAK2 and JAK3, we determined its potency against the final family member TYK2, under high ATP conditions. Pleasingly, **24** also showed no activity (>30 μM) against TYK2. With a compound in hand that we were confident had ~1000 fold selectivity over closely related family members, we were

interested in assessing its broader kinase selectivity. As such, we screened it against a panel of 386 kinases at a single concentration (1 μM). The kinome profile of compound **24** is available as Supporting Information (**Table 8**). In line with our in-house data, **24** displayed 100 % inhibition at 1 μM for JAK1, while appearing far less active against JAK2 (31 %) and JAK3 (46 %). For all other kinases tested, only PRKD1 (73 %), NUAK1 (71 %) and LRRK2 (71 %) displayed >70% inhibition, while 9 others showed >50% inhibition.

Pharmacokinetic Properties of 24

Having established that **24** was both a highly potent and selective JAK1 inhibitor, we performed a pharmacokinetic study in mice to evaluate its potential as an *in vivo* tool compound (Table **7**).

Table 7. Pharmacokinetic Properties of 24

dose (mg/Kg)	route	CL_{obs} (mL/min/kg)	$T_{1/2}$ (h)	V_{dss} (L/kg)	AUC (μM·h)	*F*%
3	i.v.[a]	68.7	2.4	10.3		
10	p.o.[a]		4.7		2.65	30
50	p.o.[b]		5.3		18.9	N.D.

[a] 10% HPbCD + 5% dextrose in WFI at pH 4. [b] 5% SBECD in WFI at pH 2. N. D. = not determined. For experimental details, see the Supporting Information.

While **24** displayed moderately high clearance but acceptable bioavailability at lower dose (10 mg/kg), the plasma concentrations reached at the higher oral dose of 50 mg/kg were anticipated to achieve target coverage (Free plasma concentration over cellular EC_{50}, Mouse PPB = 15 % free) for ~12 hours. We proceeded to test this theory in an *in vivo* xenograft model.

24 Demonstrates a Clear Pharmacodynamic (PD) Effect in NCI-H1975 Mouse Xenograft Model.

As previously discussed, STAT3 is a direct phosphorylation substrate of JAK1 in NCI-H1975 cells. Therefore, we measured pSTAT3 levels in tumors from an NCI-H1975 mouse xenograft model. Single doses of **24** at 1, 3, 10, 30, 50 and 100 mg/kg were given by oral gavage and animals were sacrificed at 2 h. An additional 6 h group was added for the 50 mg/kg dose. Interestingly, we observed a dose dependent decrease in pSTAT3 across the doses examined, which correlated with the plasma concentrations of **24** (**Graph 2**). In addition, after 6 h the 50 mg/kg dose showed a reduction in both the plasma concentration of **24** as well as suppression of pSTAT3 (**Graph 2**).

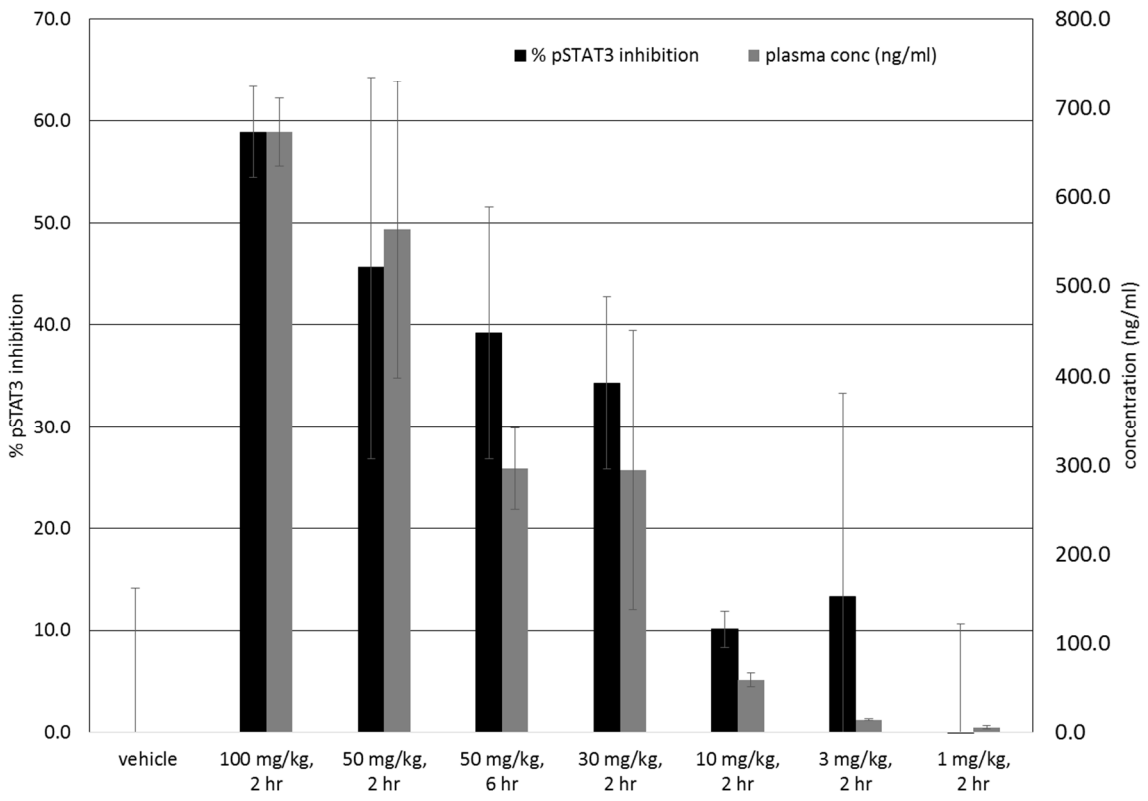

Graph 2. Plot of %inhibition of pSTAT3 in an NCI-H1975 mouse xenograft model and the corresponding plasma concentrations of **24**. Student's t-test calculated versus vehicle control; $p < 0.05$ for doses 100, 50 (2 and 6 hr), and 30 mg/kg.

Conclusion

In summary, we have described the discovery of a highly potent and selective JAK1 ATP competitive inhibitor **24**, which displays almost 1,000 fold selectivity over the highly homologous JAK family members (as determined by high ATP biochemical assays), as well as good selectivity against other kinases tested (as determined by panel screening). Compound **24** also possesses favorable PK parameters, and was demonstrated to be orally efficacious at inhibiting the phosphorylation of STAT3 in tumors in an *in vivo* model. In the future, we believe

that **24** will prove a valuable probe molecule for deconvoluting the intricacies of the JAK family biology.

Experimental Section

All reactions were performed under inert conditions (nitrogen) unless otherwise stated. Temperatures are given in degrees Celsius (°C); operations were carried out at room or ambient temperature, that is, at a temperature in the range of 18 to 25°C. All solvents and reagents were purchased from commercial sources and used without further purification. For coupling reactions, all solvents were dried and degassed prior to reaction. Reactions performed under microwave irradiation utilized either a Biotage Initiator or CEM Discover Microwave. Upon work up, organic solvents were typically dried prior to concentration with anhydrous $MgSO_4$ or Na_2SO_4. Flash silica chromatography was typically performed on an Isco Companion, using Silicycle silica gel, 230-400 mesh 40-63 μm cartridges, Grace Resolv silica cartridges or Isolute Flash Si or Si II cartridges. Reverse phase chromatography was performed using a Waters XBridge Prep C18 OBD column, 5μ silica, 19 mm diameter, 100 mm length), using decreasingly polar mixtures of either water (containing 0.2% NH4OH) and acetonitrile, or water (containing 0.1% formic acid) and acetonitrile, as eluents. Analytical LC-MS was performed on a Waters 2790 LC with a 996 PDA and 2000 amu ZQ Single Quadrupole Mass Spectrometer using a Phenomenex Gemini 50 x 2.1mm 5 μm C18 column, or UPLC-MS was performed on a Waters Acquity UPLC and Waters SQD mass spectrometer. UV detection = 210-400nm, mass spec = ESI with positive/negative switching. The column used was a Waters Acquity HSS T3, 1.8 μm, 2.1 x30 mm, at temperature 30 ^{o}C. Flow rate was 1mL/min using a solvent gradient of 2 to 98% B over 1.5 minutes (total runtime with equilibration back to starting conditions = 2 min), where A = 0.1% formic acid in water and B = 0.1% formic acid in acetonitrile. Purities were measured

by UV absorption at 254 nm or TIC and are ≥ 95% unless otherwise stated. NMR spectra were recorded on a Bruker AV300, AV400 and DRX500 spectrometer at 300 or 500 MHz at 303K unless otherwise indicated. 1H NMR spectra are reported as chemical shifts in parts per million (ppm) relative to an internal solvent reference. Yields are given for illustration only and are not necessarily those which can be obtained by diligent process development; preparations were repeated if more material was required. Purity of final compounds was assessed by reversed-phase UHPLC with UV diode array detection at 210-400 nM; all tested compounds were >95% purity.

General Procedure: Displacement of C-2 Pyrimidine Chlorides with Anilines

To an alcoholic solution (0.128 mmol) of 5-subsituted (3-((2-chloropyrimidin-4-yl)(methyl)amino)phenyl)methanol (1.2 eq) in a microwave reaction vessel was added 3-(4-methylpiperazin-1-yl)-5-(methylsulfonyl)aniline (1 eq), and acid (3 eq) and heated to 80-125 °C in a microwave for 1-2 h. Solvent was evaporated under reduced pressure and the resultant residue was partitioned between ethyl acetate and sat. NaHCO3 aq. The organic layer was taken, washed with brine, and dried over MgSO4, filtered and evaporated. The residue was purified as indicated per example.

N^4-(3-chloro-2,4-difluorophenyl)-N2-(3-(4-methylpiperazin-1-yl)-5-(methylsulfonyl)phenyl)pyrimidine-2,4-diamine (3).

Scale: 0.56 mmol. Acid: pTSA. Solvent: IPA. Temp: 125 °C. Time: 1 h. Purification column chromatography (silica gel, 0-2% MeOH (1% 7M NH_3 in MeOH)/DCM). Sample: **3** as a light brown solid (25 mg, 14%); ^{1}H NMR (300 MHz, DMSO-*d6*) δ 9.14 - 9.42 (m, 2 H), 8.10 (d, 1 H), 7.91 - 8.07 (m, 1 H), 7.70 (s, 1 H), 7.56 (s, 1 H), 7.26 (td, 1 H), 6.92 (s, 1 H), 6.37 (d, 1 H), 2.96 -

3.17 (m, 8 H), 2.35 - 2.44 (m, 3 H), 2.21 (s, 3 H); *m/z* (ES+) $(M+H)^+$ = 509.13.

(3-(2-(3,5-Dimorpholinophenylamino)-5-methylpyrimidin-4-ylamino)phenyl)methanol (4).

Scale: 0.20 mmol. Acid: HCl, 1.25 M in MeOH. Solvent: EtOH. Temp: 100 °C. Time: 3 h. Purification: column chromatography (silica gel, 0-2% MeOH (1% 7M NH_3 in MeOH)/DCM). Sample: **4** as an off white solid (38 mg, 14%); ^{1}H NMR (300 MHz, DMSO-*d6*) δ 8.63 (s, 1 H), 8.22 (s, 1 H), 7.88 (s, 1 H), 7.65 (s, 1 H), 7.55 (s, 1 H), 7.21 (t, 1 H), 6.97 (d, 1 H), 6.84 (s, 2 H), 6.02 (s, 1 H), 5.12 (t, 1 H), 4.46 (d, 2 H), 3.56 - 3.68 (m, 8 H), 2.83 - 2.95 (m, 8 H), 2.08 (s, 3 H); *m/z* (ES+) $(M+H)^+$ = 477.26.

(3-(2-(3-(4-Methylpiperazin-1-yl)-5-(methylsulfonyl)phenylamino)pyrimidin-4-ylamino)phenyl)methanol (5).

Scale: 0.26 mmol. Acid: HCl, 2M in diethyl ether. Solvent: EtOH. Temp: 80 °C. Time: 2.5 h. Purification: reverse-phase chromatography (25-35% MeCN/H_2O 0.2% NH_4OH, 4 min). Sample: **5** as an off-white solid (5 mg, 4%); ^{1}H NMR (300 MHz, DMSO-*d6*) δ 9.31 (br. s., 1 H), 9.22 (br. s., 1 H), 7.98 (d, 1 H), 7.66 - 7.90 (m, 2H), 7.62 (s, 1 H), 7.38 (s, 1 H), 7.20 (t, 1 H), 6.73 - 7.04 (m, 2 H), 6.21 (d, 1 H), 5.08 (br. s., 1 H), 4.42 (s, 2 H), 3.07 (m, 7 H), 2.36 (m, 4 H), 2.12 (s, 3 H); *m/z* (ES+) $(M+H)^+$ = 469.31.

(3-(5-fluoro-2-(3-(4-methylpiperazin-1-yl)-5-(methylsulfonyl)phenylamino)pyrimidin-4-ylamino)phenyl)methanol (6).

Scale: 0.48 mmol. Acid: HCl, 1.25 M in MeOH. Solvent: EtOH. Temp: 120 °C. Time: 0.5 h. Purification: reverse-phase chromatography (30-60% MeCN/H_2O 0.2% NH_4OH, 10 min). Sample: **6** as an off-white solid (100 mg, 43%); ^{1}H NMR (300 MHz, DMSO-*d6*) δ 9.23 - 9.48 (m, 2 H), 8.16 (d, 1 H), 7.79 (d, 1 H), 7.55 - 7.73 (m, 3 H), 7.29 (t, 1 H), 7.04 (d, 1 H), 6.94 (s, 1

H), 5.15 (br. s., 1 H), 4.50 (s, 2 H), 2.94 - 3.27 (m, 8 H), 2.40 (m, 3 H), 2.21 (s, 3 H); *m/z* (ES+) $(M+H)^+$ = 487.21.

(3-(5-methyl-2-(3-(4-methylpiperazin-1-yl)-5-(methylsulfonyl)phenylamino)pyrimidin-4-ylamino)phenyl)methanol (7).

Scale: 4.00 mmol. Acid: HCl, 1.25 M in MeOH. Solvent: EtOH. Temp: 120 °C. Time: 2 h. Purification: reverse-phase chromatography (20-40% MeCN/H_2O 0.2% NH_4OH, 10 min). Sample: **7** as an off-white solid (0.70 g, 36%). ^{1}H NMR (300 MHz, DMSO-*d6*) δ 9.14 (s, 1 H), 8.29 (s, 1 H), 7.95 (s, 1 H), 7.63 - 7.81 (m, 3 H), 7.57 (s, 1H), 7.26 (t, 1 H), 6.99 (d, 1 H), 6.89 (s, 1 H), 5.13 (t, 1 H), 4.49 (d, 2 H), 2.95 - 3.15 (m, 8 H), 2.40 (s, 3 H), 2.21 (s, 3 H), 2.13 (s, 3 H); *m/z* (ES+) $(M+H)^+$ = 483.21.

(3-(5-chloro-2-(3-(4-methylpiperazin-1-yl)-5-(methylsulfonyl)phenylamino)pyrimidin-4-ylamino)phenyl)methanol (8).

Scale: 0.56 mmol. Acid: HCl, 1.25 M in MeOH. Solvent: EtOH. Temp: 120 °C. Time: 0.5 h. Purification: reverse-phase chromatography (20-60% MeCN/H_2O 0.2% NH_4OH, 10 min). Sample: **8** as an off-white solid (0.14 g, 51%); ^{1}H NMR (300 MHz, DMSO-*d6*) δ 9.09 (s, 1 H), 8.69 (s, 1 H), 7.89 (s, 2 H), 7.76 (s, 1 H), 7.68 (s, 2 H), 7.27 (t, 1 H), 7.01 (d, 1 H), 6.89 (s, 1 H), 5.11 (t, 1 H), 4.49 (d, 2 H), 3.88 (s, 3 H), 3.03 - 3.21 (m, 4 H), 2.42 (m, 4 H), 2.22 (s, 3 H); *m/z* (ES+) $(M+H)^+$ = 503.13.

(3-(5-Bromo-2-(3-(4-methylpiperazin-1-yl)-5-(methylsulfonyl)phenylamino)pyrimidin-4-ylamino)phenyl)methanol (9).

Scale: 0.37 mmol. Acid: HCl, 1.25 M in MeOH. Solvent: EtOH. Temp: 125 °C. Time: 1 h. Purification: reverse-phase chromatography (20-60% MeCN/H_2O 0.2% NH_4OH, 10 min).

Sample: **9** as an off-white solid (109 mg, 54%); ^{1}H NMR (300 MHz, DMSO-*d6*) δ 9.44 (s, 1 H) 8.55 (s, 1 H) 8.29 (s, 1 H) 7.55 - 7.77 (m, 3 H) 7.51 (s, 1H) 7.29 (t, 1 H) 7.07 (d, 1 H) 6.94 (s, 1 H) 4.97 - 5.29 (m, 1 H) 4.48 (d, 2 H) 2.93 - 3.14 (m, 8 H) 2.31 - 2.43(m, 3 H) 2.21 (s, 3 H); *m/z* (ES+) $(M+H)^+$ = 548.8.

(3-(5-Methyl-2-(3-(methylsulfonyl)-5-morpholinophenylamino)pyrimidin-4-ylamino)phenyl)methanol (10).

Scale: 0.56 mmol. Acid: HCl, 1.25 M in MeOH. Solvent: EtOH. Temp: 125 °C. Time: 0.5 h. Purification: column chromatography (silica gel, 0-3% MeOH/DCM). Sample: **10** as an off-white solid (115 mg, 63%); ^{1}H NMR (300 MHz, DMSO-*d6*) δ 9.19 (s, 1 H), 8.31 (s, 1 H), 7.95 (s, 1 H), 7.60 - 7.80 (m, 3 H), 7.55 (s, 1 H), 7.26 (t, J = 7.82 Hz, 1 H), 7.00 (d, 1 H), 6.89 (s, 1 H), 5.13 (t, 1 H), 4.49 (d, 2 H), 3.53 - 3.77 (m, 4 H), 3.11 (s, 3 H), 2.87 - 3.06 (m, 4 H), 2.13 (s, 3 H); *m/z* (ES+) $(M+H)^+$ = 470.3.

(3-(5-Methyl-2-(3-(4-methylpiperazin-1-yl)phenylamino)pyrimidin-4-ylamino)phenyl)methanol (11).

Scale: 0.34 mmol. Acid: HCl, 2 M in diethyl ether. Solvent: TFE. Temp: 160 °C. Time: 1 h. Purification: reverse-phase chromatography (20-50% MeCN/H_2O 0.2% NH_4OH, 5 min). Sample: **11** as an off-white solid (70 mg, 50%); ^{1}H NMR (300 MHz, DMSO-*d6*) δ 8.73 (s, 1 H), 8.22 (s, 1 H), 7.88 (s, 1 H), 7.67 (d, 1 H), 7.59 (s, 1 H), 7.17 - 7.29 (m, 3 H), 6.94 - 7.03 (m, 2 H), 6.45 (dd, 1 H), 5.12 (t, 1 H), 4.49 (d, 2 H), 2.91 - 3.03 (m, 4 H), 2.35 - 2.42 (m, 4 H), 2.20 (s, 3 H), 2.10 (s, 3 H); *m/z* (ES+) $(M+H)^+$ = 403.2.

(3-(5-methyl-2-(3-(methylsulfonyl)-5-(piperazin-1-yl)phenylamino)pyrimidin-4-ylamino)phenyl)methanol (12).

Scale: 0.51 mmol. Acid: HCl, 1.25 M in MeOH. Solvent: EtOH. Temp: 110 °C. Time: 1 h. Purification: column chromatography (silica gel, 0-10% MeOH (1% 7M NH_3 in MeOH)/DCM). Sample: **12** as an off white solid (38 mg, 14%); ^{1}H NMR (300 MHz, DMSO-*d6*) δ 9.13 (s, 1 H), 8.29 (s, 1 H), 7.95 (d, 1 H), 7.75 (d, 1 H), 7.61 - 7.72 (m, 2H), 7.57 (s, 1 H), 7.26 (t, 1 H), 7.00 (d, 1 H), 6.87 (d, 1 H), 5.13 (br. s., 1 H), 4.49 (s, 2 H), 2.92 - 3.20 (m, 7 H), 2.65 - 2.88 (m, 4H), 2.00 - 2.17 (m, 3 H); *m/z* (ES+) $(M+H)^+$ = 509.13.

(3-(2-(3-((cis)-3,5-dimethylpiperazin-1-yl)-5-(methylsulfonyl)phenylamino)-5-methylpyrimidin-4-ylamino)phenyl)methanol (13).

To a suspension of 3-(2-chloro-5-methylpyrimidin-4-ylamino)phenyl)methanol (0.10 g, 0.40 mmol), 3-((cis)-3,5-dimethylpiperazin-1-yl)-5-(methylsulfonyl)aniline (113 mg, 0.40 mmol) and Cs_2CO_3 (0.39 g, 1.20 mmol) in 1,4-dioxane (2 mL) were added tris(dibenzylideneacetone)dipalladium (0) (37 mg, 0.04 mmol) and 2-dicyclohexylphosphino-2',4',6'-triisopropylbiphenyl (57 mg, 0.12 mmol) and sealed under a nitrogen atmosphere. The resultant reaction mixture was stirred at 100 °C under nitrogen overnight. The reaction mixture was cooled to room temperature, diluted with DCM and filtered. The filtrate was concentrated to dryness and purified by column chromatography (silica, 0-10% MeOH/DCM) to afford **13** as an off-white solid (47 mg, 23%); ^{1}H NMR (300 MHz, DMSO-*d6*) δ 9.13 (s, 1 H), 8.27 (br s, 1H), 7.95 (s, 1 H), 7.79 (s, 1 H), 7.71 (s, 1 H), 7.62 (d, 2 H), 7.26 (t, 1 H), 6.99 (d, 1 H), 6.90 (s, 1 H), 5.11 (s, 1 H), 4.49 (d, 2 H), 3.45 (d, 2 H), 3.11 (s, 3 H), 2.71 - 2.84 (m, 2 H), 2.04 - 2.17 (m, 5 H), 0.98 (d, J = 6.22 Hz, 6 H); *m/z* (ES+) $(M+H)^+$ = 497.26.

1-(4-(3-(4-(3-(hydroxymethyl)phenylamino)-5-methylpyrimidin-2-ylamino)-5-(methylsulfonyl)phenyl)piperazin-1-yl)ethanone (14).

To a suspension of 3-(2-chloro-5-methylpyrimidin-4-ylamino)phenyl)methanol (0.10 mg, 0.40 mmol), 1-(4-(3-amino-5-(methylsulfonyl)phenyl)piperazin-1-yl)ethanone (0.12 mg, 0.40 mmol) and Cs_2CO_3 (0.39 g, 1.20 mmol) in 1,4-dioxane (2 mL) were added tris(dibenzylideneacetone)dipalladium (0) (37 mg, 0.04 mmol) and 2-dicyclohexylphosphino-2',4',6'-triisopropylbiphenyl (57 mg, 0.12 mmol) and sealed under a nitrogen atmosphere. The resultant reaction mixture was stirred at 100 °C. The reaction mixture was cooled to room temperature, diluted with DCM and filtered. The filtrate was concentrated to dryness and purified by column chromatography (silica gel, 0-40% MeOH/DCM) to afford **14** as a cream-colored solid (0.11 g, 96%); ^{1}H NMR (300 MHz, DMSO-*d6*) δ 9.19 (s, 1 H), 8.32 (s, 1 H), 7.95 (s, 1 H), 7.68 - 7.76 (m, 2 H), 7.65 (s, 1 H), 7.56 (s, 1 H), 7.26 (t, 1 H), 7.00 (d, 1 H), 6.92 (s, 1 H), 5.13 (t, 1 H), 4.49 (d, 2 H), 3.50 (s, 4 H), 3.11 (s, 3 H), 2.97 - 3.10 (m, 4 H), 2.13 (s, 3 H), 2.04 (s, 3 H); *m/z* (ES+) $(M+H)^+$ = 511.08.

-(4-(3-(4-(3-(hydroxymethyl)phenylamino)pyrimidin-2-ylamino)-5-(methylsulfonyl)phenyl)piperazin-1-yl)ethanol (15).

Scale: 0.40 mmol. Acid: HCl, 1.25 M in MeOH. Solvent: EtOH. Temp: 80 °C. Time: 2.5 h. Purification: column chromatography (silica gel, 0-10% MeOH/ DCM). Sample: **15** as an off-white solid (12 mg, 6%); ^{1}H NMR (300 MHz, DMSO-*d6*) δ 9.18 (s, 1 H), 8.32 (s, 1 H), 7.95 (s, 1 H), 7.65 - 7.77 (m, 3 H), 7.56 (s, 1 H), 7.26 (t, 1 H), 7.00 (d, 1 H), 6.87 - 6.95 (m, 1 H), 5.12 - 5.21 (m, 1 H), 4.46 - 4.54 (m, 2 H), 3.52 - 3.75 (m, 2 H), 2.96 - 3.26 (m, 8 H), 2.67 (m, J = 2.00 Hz, 2 H), 2.52 - 2.64 (m, 3 H), 2.12 (s, 3 H); *m/z* (ES+) $(M+H)^+$ = 513.18.

(3-(2-(3-(4-(2-Methoxyethyl)piperazin-1-yl)-5-(methylsulfonyl)phenylamino)-5-methylpyrimidin-4-ylamino)phenyl)methanol (16).

Scale: 0.38 mmol. Acid: HCl, 1.25 M in MeOH. Solvent: IPA. Temp: 125 °C. Time: 1 h. Purification: column chromatography (silica gel, 0-3% MeOH/DCM over 35 min). Sample: **16** as an off-white solid (55 mg, 33%); ^{1}H NMR (300 MHz, DMSO-*d6*) δ 7.89 (s, 1 H), 7.61 - 7.70 (m, 2 H), 7.48 - 7.57 (m, 2 H), 7.31 (t, 1 H), 7.10 (d, 1 H), 6.98 - 7.05 (m, 1 H), 4.59 (s, 2 H), 3.58 (t, 2 H), 3.36 (s, 3 H), 3.07 - 3.14 (m, 4 H), 3.05 (s, 3 H), 2.62 (dt, 6 H), 2.17 (s, 3 H); *m/z* (ES+) $(M+H)^+$ = 527.19.

(3-(5-methyl-2-(3-((1*S*,4*S*)-5-methyl-2,5-diazabicyclo[2.2.1]heptan-2-yl)-5-(methylsulfonyl)phenylamino)pyrimidin-4-ylamino)phenyl)methanol (17).

Scale: 0.22 mmol. Acid: HCl, 1.25 M in MeOH. Solvent: EtOH. Temp: 90 °C. Time: 1 h. Purification: column chromatography (silica gel, 0-10% MeOH/DCM). Sample: **17** as an off-white solid (34 mg, 38%); ^{1}H NMR (300 MHz, DMSO-*d6*) δ 9.01 (s, 1 H), 8.22 (s, 1 H), 7.86 (s, 1 H), 7.64 (d, 1 H), 7.49 (s, 1H), 7.39 (s, 1 H), 7.30 (s, 1 H), 7.19 (t, 1 H), 6.93 (d, 1 H), 6.44 (s, 1 H), 5.13 (br. s., 1 H), 4.41 (s, 2 H), 3.94 (br. s., 1 H), 3.31 (br. s., 1 H), 2.93 - 3.11 (m, 4 H), 2.63 (d, 1 H), 2.37 (d, 1 H), 2.12 - 2.24 (m, 3 H), 1.93 - 2.11 (m, 3 H), 1.53 - 1.83 (m, 3 H); *m/z* (ES+) $(M+H)^+$ = 495.23.

General Procedure: Displacement of C-4 Anilino-Pyrimidine Chlorides with Anilines

To a suspension of 4-chloro-pyrimidine (1 eq) in TFE (0.1 M) was added (3-aminophenyl) methanol (1.1 eq), and 4M HCl in 1,4-Dioxane (4 eq) and heated to 150 °C in a microwave for 1 h. The reaction was cooled to room temp and solvent removed under reduced pressure. The residue was purified as indicated per example.

(3-(2-(3-(Difluoromethyl)-5-((1*S*,4*S*)-5-methyl-2,5-diazabicyclo[2.2.1]heptan-2-yl)phenylamino)-5-methylpyrimidin-4-ylamino)phenyl)methanol (18).

Scale: 0.1 mmol. Purification: reverse-phase chromatography (40-60% MeCN/H_2O 0.2% NH_4OH, 10 min). Sample: **18** as an off-white solid (25 mg, 51%); ^{1}H NMR (300 MHz, MeOH-*d4*) δ 7.87 (s, 1 H) 7.62 - 7.71 (m, 1 H) 7.45 - 7.62 (m, 1 H) 7.34 (t, 1 H) 7.15 (dd, 1.70 Hz, 2 H) 6.99 (s, 1 H) 6.51 (s, 1 H) 6.20 - 6.42 (m, 1 H) 4.60 (s, 2 H) 4.03 (s, 1 H) 3.52 (s, 1 H) 3.12 - 3.30 (m, 2 H) 2.60 - 2.85 (m, 2 H) 2.39 (s, 3H) 2.09 - 2.23 (m, 3 H) 1.63 - 2.01 (m, 2 H); *m/z* (ES+) $(M+H)^+$ = 467.3.

3-(2-(3-(Difluoromethyl)-2-fluoro-5-((1*S*,4*S*)-5-methyl-2,5-diazabicyclo[2.2.1]heptan-2-yl)phenylamino)-5-methylpyrimidin-4-ylamino)phenyl)methanol (19).

Scale: 0.1 mmol. Purification: reverse-phase chromatography (30-50% MeCN/H_2O 0.2% NH_4OH, 5 min). Sample: **19** as an off-white solid (26 mg, 53%); ^{1}H NMR (300 MHz, DMSO-*d6*) δ 8.25 (d, 2 H), 7.87 (d, J = 0.75 Hz, 1 H), 7.62 (d, 1 H), 7.55 (s, 1 H), 7.19 - 7.25 (m, 1 H), 7.16 (t, 1 H), 7.06 (t, 1H), 6.95 (d, 1 H), 6.27 - 6.37 (m, 1 H), 5.15 (br. s., 1 H), 4.41 (s, 2 H), 3.95 (s, 1 H), 3.36 (br. s., 1 H), 3.10 (d, 1 H), 2.97 (d, 1 H), 2.65 (d, 1 H), 2.37 - 2.45 (m, 1 H), 2.22 (s, 3 H), 2.09 (s, 3 H), 1.79 (d, 1 H), 1.70 (d, J = 8.85 Hz, 1 H); *m/z* (ES+) $(M+H)^+$ = 485.1.

(3-(2-(2-Fluoro-5-((1*S*,4*S*)-5-methyl-2,5-diazabicyclo[2.2.1]heptan-2-yl)pyridin-3-ylamino)-5-methylpyrimidin-4-ylamino)phenyl)methanol (20).

Scale: 0.43 mmol. Purification: reverse-phase chromatography (20-40% MeCN/H_2O 0.2% NH_4OH, 10 min). Sample: **20** as an off-white solid (95 mg, 51%); ^{1}H NMR (300 MHz, DMSO-*d6*) δ 8.29 (s, 1 H), 8.23 (s, 1 H), 7.89 (d, 1 H), 7.62 (dd, 1 H), 7.53 - 7.60 (m, 2 H), 7.19 (t, 1

H), 7.05 (t, 1 H), 6.98 (d, 1 H), 5.14 (t, 1 H), 4.43 (d, 2 H), 3.91 (s, 1 H), 3.27 - 3.36 (m, 1 H), 3.07 (dd, 1 H), 2.94 (d, 1 H), 2.61 (dd, 1 H), 2.38 (d, 1 H), 2.19 (s, 3 H), 2.09 - 2.14 (m, 3 H), 1.73 - 1.81 (m, 1 H), 1.63 - 1.71 (m, 1 H); *m/z* (ES+) $(M+H)^+$ = 436.2.

General Procedure: Displacement of C-4 Anilino-Pyrimidine Chlorides with Alkyl Amines

To a suspension of 4-chloro-N-(2-fluoro-5-((1*S*,4*S*)-5-methyl-2,5-diazabicyclo[2.2.1]heptan-2-yl)pyridin-3-yl)-5-methylpyrimidin-2-amine (1 eq) in butan-1-ol (0.25 M) was added alkyl amine (3 eq) and DIPEA (2 eq) and the reaction heated to 125 °C for 24 h. Reaction mixture evaporated and the residue was purified as indicated per example.

***N*2-(2-fluoro-5-((1*S*,4*S*)-5-methyl-2,5-diazabicyclo[2.2.1]heptan-2-yl)pyridin-3-yl)-5-methyl-*N*4-(pentan-3-yl)pyrimidine-2,4-diamine (22).**

Scale: 0.43 mmol. Purification: reverse-phase chromatography (40-50% MeCN/H_2O 0.2% NH_4OH, 10 min). Sample: **22** as an off-white solid (0.12 g, 73%); ^{1}H NMR (300 MHz, DMSO-*d6*) δ 7.96 (dd, 1 H), 7.81 (s, 1 H), 7.65 (d, 1 H), 7.01 (t, 1 H), 6.16 (d, 1 H), 4.21 (s, 1 H), 4.03 - 4.16 (m, 1 H), 3.41 (s, 1 H), 3.30 – 3.36 (m, 2 H), 2.77 (dd, 1 H), 2.43 - 2.49 (m, 1 H), 2.24 (s, 3 H), 1.91 - 1.99 (m, 3 H), 1.87 (d, 1 H), 1.77 (d, 1 H), 1.42 - 1.63 (m, 4 H), 0.76 - 0.87 (m, 6 H); *m/z* (ES+) $(M+H)^+$ = 400.3.

***N*2-(2-fluoro-5-((1*S*,4*S*)-5-methyl-2,5-diazabicyclo[2.2.1]heptan-2-yl)pyridin-3-yl)-5-methyl-*N*4-((*R*)-3-methylbutan-2-yl)pyrimidine-2,4-diamine (23).**

Scale: 0.43 mmol. Purification: reverse-phase chromatography (40-50% MeCN/H_2O 0.2% NH_4OH, 10 min). Sample: **23** as an off-white solid (0.13 g, 76%); ^{1}H NMR (300 MHz, DMSO-*d6*) δ 7.91 (dd, 1 H), 7.84 (s, 1 H), 7.65 (d, 1 H), 7.02 (t, 1 H), 6.15 (d, 1 H), 4.22 (s, 1 H), 3.93 - 4.10 (m, 1 H), 3.41 (s, 1 H), 3.33 (m, 1 H), 3.15 (d, 1 H), 2.77 (dd, 1 H), 2.43 - 2.49 (m, 1 H), 2.24 (s, 3 H), 1.94 (s, 3 H), 1.72 - 1.90 (m, 3 H), 1.12 (d, 3 H), 0.87 (dd, 6 H); *m/z* (ES+) $(M+H)^+$ = 400.4.

***N*2-(2-fluoro-5-((1*S*,4*S*)-5-methyl-2,5-diazabicyclo[2.2.1]heptan-2-yl)pyridin-3-yl)-5-methyl-*N*4-((*R*)-butan-2-yl)pyrimidine-2,4-diamine (24).**

Scale: 24.83 mmol. Purification: reverse-phase chromatography (35-50% MeCN/H_2O 0.2% NH_4OH, 15 min). Sample: **24** as a beige crystalline solid (6.63 g, 69%); ^{1}H NMR (300 MHz, DMSO-*d6*) δ 7.95 (dd, J = 9.06, 2.83 Hz, 1 H), 7.83 (s, 1 H), 7.65 (d, 1 H), 7.01 (t, 1 H), 6.25 (d, 1 H), 4.21 (s, 1 H), 4.09 - 4.19 (m, 1 H), 3.41 (s, 1 H), 3.29 (m, 1 H), 3.15 (d, 1 H), 2.77 (dd, 1 H), 2.40 - 2.48 (m, 1 H), 2.24 (s, 3 H), 1.90 - 1.97 (m, 3 H), 1.87 (d, 1 H), 1.77 (d, 1 H), 1.41 - 1.66 (m, 2 H), 1.15 (d, 3 H), 0.85 (t, 3 H); *m/z* (ES+) $(M+H)^+$ = 386.3.

ASSOCIATED CONTENT

Supporting Information

This material is available free of charge via the Internet at http://pubs.acs.org.

Protocols for the enzyme and cell assays, synthetic methods, crystallographic information, molecular formula strings, and kinase panel selectivity data for compound **24** in Table 8.

AUTHOR INFORMATION

Corresponding Author

*Tel.: + +1 781-839-4175. E-mail: neil.grimster@astrazeneca.com.

Present Addresses

†If an author's address is different than the one given in the affiliation line, this information may be included here.

Author Contributions

The manuscript was written through contributions of all authors. All authors have given approval to the final version of the manuscript.

Notes

The authors declare no competing financial interest.

ACKNOWLEDGMENT

We thank A. Hird for proofreading the manuscript and helpful discussions.

ABBREVIATIONS

EGFR, epidermal growth factor receptor; MAPK, mitogen-activated protein kinase; Akt, protein kinase B; STAT, signal transducer and activator of transcription; ATP, adenosine triphosphate; EphB4, Ephrin type-B receptor 4; Phe, phenylalanine; Leu, leucine; Met, methionine; Asp,

aspartic acid; Asn, asparagine; Glu, glutamic acid; Arg, arginine; HPBCD, 2-hydroxypropyl-beta-cyclodextrin; wfi, water for injection; SBECD, sulfobutylether-β-cyclodextrin.

ANIMAL EXPERIMENTS: All experimental activities involving animals were carried out in accordance with AstraZeneca animal welfare protocols, which are consistent with The American Chemical Society Publications rules and ethical guidelines.

PDB ID CODE: **6ELR**. Authors will release the atomic coordinates and experimental data upon article publication.

References

(1) Vakil, E.; Tefferi, A. BCR-ABL1-negative myeloproliferative neoplasms: a review of molecular biology, diagnosis, and treatment. *Clin Lymphoma Myeloma Leuk* **2011**, *11*, S37-S45.

(2) Kiu, H.; Nicholson, S. E. Biology and significance of the JAK/STAT signalling pathways. *Growth Factors* **2012,** *30*, 88-106.

(3) Flanagan, M. E.; Blumenkopf, T. A.; Brissette, W. H.; Brown, M. F.; Casavant, J. M.; Shang-Poa, C.; Doty, J. L.; Elliott, E. A.; Fisher, M. B.; Hines, M.; Kent, C.; Kudlacz, E. M.; Lillie, B. M.; Magnuson, K. S.; McCurdy, S. P.; Munchhof, M. J.; Perry, B. D.; Sawyer, P. S.; Strelevitz, T. J.; Subramanyam, C.; Sun, J.; Whipple, D. A.; Changelian, P. S.; Discovery of CP-690,550: A potent and selective janus kinase (JAK) inhibitor for the treatment of autoimmune diseases and organ transplant rejection. *J. Med. Chem.*, **2010**, *53*, 8468–8484.

(4) Verstovsek, S.; Kantarjian, H.; Mesa, R. A.; Pardanani, A. D.; Cortes-Franco, J.; Thomas, D. A.; Estrov, Z.; Fridman, J. S.; Bradley, E. C.; Erickson-Viitanen, S.; Vaddi, K.; Levy, R.; Tefferi,

A. Safety and efficacy of INCB018424, a JAK1 and JAK2 inhibitor, in myelofibrosis. *N. Engl. J. Med.* **2010**, *363*, 1117-1127.

(5) (a) Kettle, J. G.; Åstrand, A.; Catley, M.; Grimster, N. P.; Nilsson, M.; Su, Q.; Woessner, R. Inhibitors of JAK-family kinases: an update on the patent literature, part 1. *Expert Opinion on Therapeutic Patents* **2016**, *27*, 127-143. (b) Kettle, J. G.; Åstrand, A.; Catley, M.; Grimster, N. P.; Nilsson, M.; Su, Q.; Woessner, R. Inhibitors of JAK-family kinases: an update on the patent literature, part 2. *Expert Opinion on Therapeutic Patents* **2016**, *27*, 145-161. (c) Vazquez, M. L.; Kaila, N.; Strohbach, J. W.; Trzupek, J. D.; Brown, M. F.; Flanagan, M. E.; Mitton-Fry, M. J.; Johnson, T. A.; TenBrink, R. E.; Arnold, E. P.; Basak, A.; Heasley, S. E.; Kwon, S.; Langille, J.; Parikh, M. D.; Griffin, S. H.; Casavant, J. M.; Duclos, B. A.; Fenwick, A. E.; Harris, T. M.; Han, S.; Caspers, N.; Dowty, M. E.; Yang, X.; Banker, M. E.; Hegen, M.; Symanowicz, P. T.; Li, L.; Wang, L.; Lin, T. H.; Jussif, J.; Clark, J. D.; Telliez, J.-B.; Robinson, R. P.; Unwalla, R. Identification of *N*-{cis-3-[Methyl(7H-pyrrolo[2,3-d]pyrimidin-4-yl)amino]cyclobutyl}propane-1-sulfonamide (PF-04965842): a selective JAK1 clinical candidate for the treatment of autoimmune diseases. *J. Med. Chem.* **2018**, *61*, 1130-1152.

(6) (a) Menet, C. J.; Van Rompaey, L.; Geney, R. Advances in the discovery of selective JAK inhibitors. *Prog. Med. Chem.* **2013**, *52*, 153−223. (b) Menet, C.; Mammoliti, O.; Lopez-Ramos, M. Progress toward JAK1-selective inhibitors. *Future Med. Chem.* **2015**, *7*, 203−235.

(7) (a) Tan, F. H.; Putoczki, T. L.; Stylli, S. S.; Luwor, R. B. The role of STAT3 signaling in mediating tumour resistance to cancer therapy. *Curr Drug Targets* **2014**, *15*, 1341-1353. (b) Sansone, P.; Bromberg, J. Targeting the interleukin-6/Jak/Stat pathway in human malignancies. *J Clin Oncol* **2012**, *30*, 1005-1014.

(8) Lam, L.T.; Wright, G.; Davis, R. E. Cooperative signaling through the signal transducer and actrivator of transcription 3 and nuclear factor-κB pathways in subtypes of diffuse large B-cell lymphoma. *Blood* **2008**, *111*, 3701-3713.

(9) Song, J. I.; Grandis, J. R. STAT signaling in head and neck cancer. *Oncogene* **2000**, *19*, 2489-2495.

(10) (a) Turkson. J.; Jove. R. STAT proteins: novel molecular targets for cancer drug discovery. *Oncogene*. **2000**, *19*, 6613–6626. (b) Huang, M.; Page, C.; Reynolds, R. K.; Lin. J. Constitutive activation of stat 3 oncogene product in human ovarian carcinoma cells. *Gynecol Oncol.* **2000**, *79*, 67–73. (c) Niu, G.; Bowman, T.; Huang.; M..; Shivers, S.; Reintgen, D.; Daud, A.; Chang, A.; Kraker, A.; Jove, R.; Yu, H. Roles of activated Src and Stat3 signaling in melanoma tumor cell growth. *Oncogene* **2002,** *21*, 7001–7010. (d) Horiguchi, A.; Oya, M.; Shimada, T.; Uchida, A.; Marumo K.; Murai, M. Activation of signal transducer and activator of transcription 3 in renal cell carcinoma: a study of incidence and its association with pathological features and clinical outcome. *J Urol.* **2002**, *168*, 762–765. (e) Zamo, A.; Chiarle, R.; Piva, R.; Howes, J.; Fan Y.; Chilosi M.; Levy, D. E.; Inghirami, G. Anaplastic lymphoma kinase (ALK) activates Stat3 and protects hematopoietic cells from cell death. *Oncogene* **2002**, *21*, 1038–1047. (f) Corvinus, F. M.; Orth, C.; Moriggl, R.; Tsareva, S. T.; Wagner, S.; Pfitzner, E. B.; Baus, D.; Kaufmann, R.; Huberb, L. a.; Zatloukal, K.; Beug, H.; Öhlschläger, P.; Schütz, A.; Halbhuber, K-J.; Friedrich, K. Persistent STAT3 activation in colon cancer is associated with enhanced cell proliferation and tumor growth. *Neoplasia* **2005**, *7*, 545–555. (g) Chang, K.C.; Wu, M. H.; Jones D.; Chen, F. F.; Tseng, Y. L. Activation of STAT3 in thymic epithelial tumours correlates with tumour type and clinical behaviour. *J Pathol.* **2006**, *210*, 224–233. (h) Kortylewski, M.; Jove, R.;

Yu, H. Targeting STAT3 affects melanoma on multiple fronts. *Cancer Metastasis Rev.* **2005**, *24*, 315–327.

(11) Thomas, S. J.; Snowden, J. A.; Zeidler, M. P.; Danson, S. J. The role fo JAK/STAT signalling in the pathogenesis, prognosis and treatment of solid tumours. *Br J Cancer* **2015**, *113*, 365-371.

(12) (a) Tan, F. H.; Putoczki, T.L.; Stylli, S. S.; Luwor, R. B. The role of STAT3 signaling in mediating tumour resistance to cancer therapy. *Curr Drug Targets* **2014**, *15*, 1341-1353. (b) Yin, Z.; Zhang, Y.; Li, Y.; Lv, T.; Liu, J.; Wang, X. Prognostic significance of STAT3 expression and its correlation with chemioresistance of non-small cell lung cancer cells. *Acta Histochemica* **2012**, *114*, 151-158. (c) Gao, S. P.; Mark, K. G.; Leslie, K. Pao, W.; Motoi, N.; Gerald W. L.; Travis W. D.; Bornmann, W.; Veach, D.; Clarkson, B.; Bromberg, J. F. Mutations in the EGFR kinase domain mediate STAT3 activation via IL-6 production in human lung adenocarcinomas. *J Clin Invest* **2007**, *117*, 3846-3856.

(13) Sun, L.; Ma, K.; Wang, H.; Xiao, F.; Gao, Y.; Zhang, W.; Wang, K.; Gao, X.; Ip, N.; Wu, Z. JAK1–STAT1–STAT3, a key pathway promoting proliferation and preventing premature differentiation of myoblasts. *J Cell Biol.* **2007**, *179*, 129-138.

(14) Kanno, H.; Kubota, Y.; Sato, T.; Arahira, M. EP 694538 1996; *Chem. Abstr.* **1996**, *124*, 289562.

(15) (a) Bardelle, C.; Cross, D.; Davenport, S.; Kettle, J. G.; Ko, E. J.; Leach, A. G.; Mortlock, A.; Read, J.; Roberts, N. J.; Robins, P.; Williams, E. J. Inhibitors of the tyrosine kinase EphB4. Part 1: structure-based design and optimization of a series of 2,4-bis-anilinopyrimidines. *Bioorg.*

Med. Chem. Lett. **2008**, *18,* 2776-2780. (b) Bardelle, C.; Cross, D.; Davenport, S.; Kettle, J. G.; Ko, E. J.; Leach, A. G.; Mortlock, A.; Read, J.; Roberts, N. J.; Robins, P.; Williams, E. J. Inhibitors of the tyrosine kinase EphB4. Part 2: structure-based discovery and optimisation of 3,5-bis substituted anilinopyrimidines. *Bioorg. Med. Chem. Lett.* **2008**, *18*, 5717-5721. (c) Bardelle, C.; Barlaam, B.; Brooks, N.; Coleman, T.; Cross, D.; Ducray, R.; Green, I.; Lambert-van der Brempt, C.; Olivier, A.; Read, J. Inhibitors of the tyrosine kinase EphB4. Part 3: identification of non-benzodioxole-based kinase inhibitors. *Bioorg. Med. Chem. Lett.* **2010**, *20*, 5717-5721. (d) Barlaam, B.; Ducray, R.; Lambert-van der Brempt, C.; Plé, P.; Bardelle, C.; Brooks, N.; Coleman, T.; Cross, D.; Kettle, J. G.; Read, J. Inhibitors of the tyrosine kinase EphB4. Part 4: discovery and optimization of a benzylic alcohol series. *Bioorg. Med. Chem. Lett.* **2011**, *21*, 2207-2211.

(16) Hyland, R.; Roe, E. G. H.; Jones, B. C.; Smith, D. A. Identification of the cytochrome P450 enzymes involved in the *N*-demethylation of sildenafil. Br J Clin Pharmacol. **2001**, *51*, 239–248.

(17) Palm, K.; Stenberg, P.; Luthman, K.; Artursson, P. Polar molecular surface properties predict the intestinal absorption of drugs in humans. *Pharmaceutical Research* **1997**, *14*, 568–571.

(18) Meanwell, N. A. Synopsis of some recent tactical application of bioisosteres in drug design. *J. Med. Chem.* **2011**, *54*, 2529–2591.

(19) Zhu, Z.; Aref, A. R.; Cohoon, T. J.; Barbie, T. U.; Imamura, Y.; Yang, S.; Moody, S. E.; Shen, R. R.; Schinzel, A. C.; Thai, T. C.; Reibel, J. B.; Tamayo, P.; Godfrey, J. T.; Qian, Z. R.; Page, A. N.; Maciag, K.; Chan, E. M.; Silkworth, W.; Labowsky, M. T.; Rozhansky, L.; Mesirov, J. P.; Gillanders, W. E.; Ogino, S.; Hacohen, N.; Gaudet, S.; Eck, M. J.; Engelman, J.

A.; Corcoran, R. B.; Wong, K.-K.; Hahn, W. C.; Barbie, D. A. Inhibition of KRAS-driven tumorigenicity by interruption of an autocrine cytokine circuit. *Cancer Discovery* **2014** DOI: 10.1158/2159-8290.CD-13-0646

(20) Data for compound 24 was previously disclosed under the name AZ-3: Woessner, R.; Bebernitz, G.; Bell, K.; Caccese, R.; Johnson, N.; Kettle, J.; Rivard, C.; Schroeder, P.; Su, Q.; Wang, H.; Ye, M.; Zheng, W.; Zinda, M.; Lyne, P.; Vasbinder, M.; Huszar, D.; Chuaqui, C. Highly selective JAK1 kinase inhibitors suppress Y705-mediated STAT3 activation in a wide range of tumor types, with reduced hematological toxicity. Proceedings of the 104th Annual Meeting of the American Association for Cancer Research; **2013** Apr 6-10; Washington, DC. Philadelphia (PA): AACR; *Cancer Res* **2013**, 73 (8 Suppl): Abstract nr 931.

Graphical Abstract: